PCCP

Accepted Manuscript

ROYAL SOCIETY OF CHEMISTRY

www.rsc.org/pccp

Physical Chemistry Chemical Physics RSCPublishing

ARTICLE

Parallel Mechanisms of Polypyrrole Self-Discharge in Aqueous Media

Cite this: DOI: 10.1039/x0xx00000x

Received 00th January 2012,
Accepted 00th January 2012

DOI: 10.1039/x0xx00000x

www.rsc.org/

H. Olsson,[a] Z. Qiu,[a] M. Strømme[a] and M. Sjödin[a]

In this report we investigate the self-discharge in a positively charged polypyrrole-cellulose composite material in water solution. Rate constants for the self-discharge reaction are determined by potential step methods and their dependence on pH, temperature and applied potential are reported. Based on the results, we propose that two fundamentally different self-discharge mechanisms operate in parallel; one of faradaic origin with a rate constant increasing exponentially with applied potential and one mechanism comprising an initial reaction of the charged polymer with hydroxide ions. The second mechanism dominates at high pH as the rate constant for this reaction increases exponentially with pH whilst the faradaic reaction dominates at low pH. With this report we hope to shed light on the complex and elusive nature of self-discharge in conducting polymers to serve as guidance for the construction of electrical energy storage devices with conducting polymer components.

Introduction

Conducting polymers have, since their discovery, been intensely researched and find widespread use in several application areas, including ion extraction and release,[1] cell culture growth,[2, 3] actuators,[4] electroresponsive membranes,[5] electromagnetic radiation shielding,[6] thin film transistors,[7] organic light emitting diods,[8] organic solar cells[9] and sensors[10, 11]. There have also been several attempts to use conducting polymers for electrical energy storage purposes. Both polyaniline and polypyrrole (PPy) have, for instance, been used as positive electrode materials against a lithium anode in the early development of lithium ion battery technologies[12-15] and more recent advances, related to morphological changes, has realized much improved rates and cycling stabilities in conducting polymer battery materials.[16-23] High self-discharge rates and low intrinsic charge storage capacities do however limit the usefulness of conducting polymers as active charge storage capacity carrying battery- or capacitor component.[24-26] The latter problem can be overcome by introducing high capacity redox active pendant groups to the polymer, thus forming a conducting redox polymer, where the pendant groups serve as charge storage components while the conducting polymer ensures material conductivity.[27-34] Self-discharge, however, must be resolved by other means. In order to enable rational design of polymer structures and cell designs, to overcome problems with self-discharge, the processes leading to charge- and/or potential loss needs to be understood on a fundamental level.

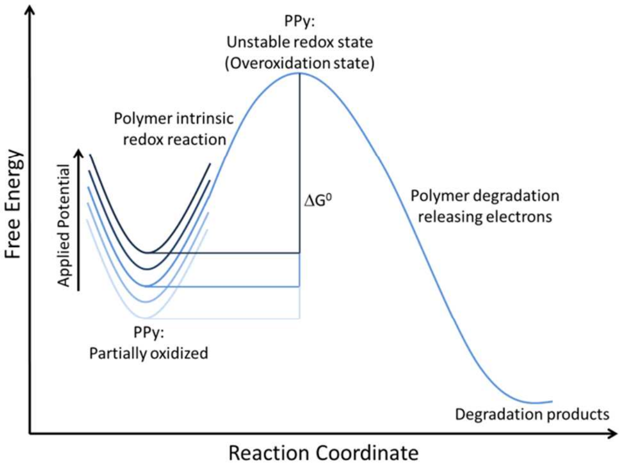

Figure 1: In its oxidized state PPy undergoes self-discharge via a reactive, polymer intrinsic, redox intermediate that reacts further in a kinetically non-limiting reaction and releases electrons thus reducing the polymer. The free energy (ΔG^0) for reaching the intermediate state is affected by the potential of the polymer and the self-discharge rate increases exponentially with potential.

To this end we have previously reported results that show that the dominant self-discharge mechanism in positively charged PPy in aqueous media is a multi-step reaction with an initial, rate limiting and polymer intrinsic redox reaction leading to an unstable intermediate state (Fig. 1).[35, 36] The rate of this reaction depends on the potential applied to the polymer. As an increased potential increases the free energy of the charged polymer, *i.e.* of the bipolaron states, relative to the redox state of the intermediate the energy required to reach the unstable redox state (ΔG^0) is decreased. Through temperature dependence data we estimated the redox potential of the intermediate to be 0.89 V *vs.* Ag/AgCl which corresponds well to the potential where the process commonly referred to as over oxidation occurs and concluded that self-discharge and over-oxidation are in-fact the same process. Furthermore, we showed that the reaction was rate limited by the formation of the intermediate state, which is a polymer intrinsic reaction, and that the follow-up reaction was much faster than the back-reaction.

Although the proposed mechanism accounts well for the observed self-discharge behaviour, the mechanism fails to describe the dependence of the self-discharge rate on the surrounding media. As pH-dependence of both polymer degradation [37-41] and self-discharge,[42, 43] has been reported by several research groups this needs to be clarified. In this study we have therefore investigated the dependence on pH of self-discharge to reach consensus regarding the seemingly conflicting results and aim to present a unifying model that brings the observations together.

Experimental

Synthesis of the PPy/cellulose composite

PPy composites were produced with cellulose from the *Cladophora sp.* Algae[44] according to previously described protocols.[45] Pyrrole (>97%) was purchased from Sigma-Aldrich while iron (III) chloride hexahydrate (>99%), Tween 80 and sodium chloride (>99.5%) were purchased from VWR international. The chemicals were used without further purification. Cellulose was dispersed in water using sonication (300 mg cellulose in 60 mL H_2O). Pyrrole and one drop of Tween 80 was dissolved in 0.5 M HCl (1.5 ml Pyrrole in 50 mL acid). An iron salt solution was prepared by dissolving iron (III) chloride in 0.5 M HCl (12.86 g $FeCl_3$ in 100 mL acid). The pyrrole solution and cellulose dispersion were then mixed, and finally the iron solution was added to start the polymerization. The reaction time was 30 minutes at room temperature. The polymer composite was then washed with 5 L of 0.5 M HCl followed by 1 L of 0.1 M NaCl. After additional sonication, the polymer composite was dried onto a filter paper in a Büchner funnel, peeled off and pressed in a vise overnight. The composite was then dried for at least three days at ambient conditions and the resulting material was a flexible, freestanding, paper-like material with a porous structure of cellulose fibres covered by a 30-50 nm layers of polypyrrole.[45]

Electrochemical measurements of self-discharge

Electrochemical experiments were carried out using an Autolab PGSTAT302N potentiostat (Ecochemie, the Netherlands) or a CH Instruments Electrochemical Workstation CHI660D (CH Instruments, USA). The self-discharge of positively charged PPy was studied in a three-electrode setup. In these experiments a coiled Pt wire was employed as the counter electrode while a 3 M NaCl Ag/AgCl electrode was used as the reference electrode. Both the counter electrode and reference electrode were placed in separate compartments, and the electrolyte was purged with nitrogen for 10 minutes prior to the start of the measurements and was thereafter kept under nitrogen. The PPy composite was connected as the working electrode with the aid of a Pt wire, folded around the sample. The electrolyte was a 1.0 M NaCl solution with 0.1 M Na_2HPO_4 and 0.1 M H_3BO_3 buffer. The pH was adjusted with HCl or NaOH.

The self-discharge was measured by taking a number of 300 s long potential steps in the interval 0.3 V to 0.6 V *vs.* Ag/AgCl (50 mV steps, 7 steps in total), and measuring the stable current at the end of each potential step. The current flowing after 300 s, when the PPy has had sufficient time to reach the applied potential, constitutes the leakage current due to self-discharge [46]. These self-discharge measurements were carried out at 7 different pH values (2.03, 3.03, 4.01, 5, 6, 7, 8) and 7 temperatures (10 °C, 20 °C, 30 °C, 40 °C, 50 °C, 60 °C, 70 °C), giving a total of 343 leakage current values. Due to a rapid degradation at high potentials, pH values and temperatures, a steady leakage current could not be obtained in some cases. In particular this limited the accessible pH-range to below pH 8 at room temperature. Each potential step was qualitatively inspected, and points without a stable current plateau were discarded and excluded from further analysis. Afterwards, a total of 189 data points remained. The leakage current was converted to a self-discharge rate, k [1/s], through equation 1

$$k = \frac{i_{leak}}{Q(E) \cdot m} \qquad (1)$$

where i_{leak} is the leakage current from the potential step, Q(E) [C/g] is the integrated charge from a CV measurement up to each potential (see ref. [36] for a more detailed explanation), and *m* is the mass of the sample.

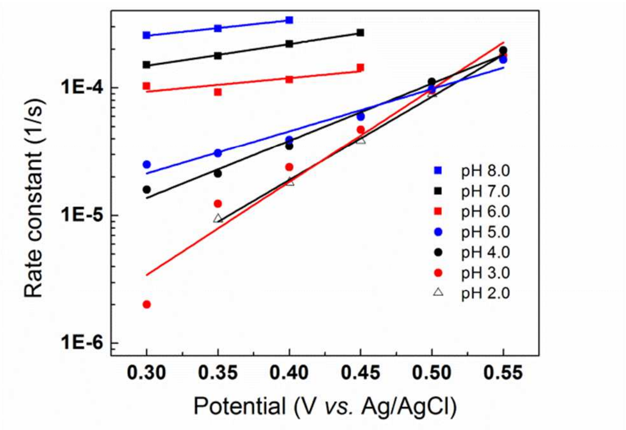

Figure 2. Rate constants for self-discharge of PPy covered cellulose fibres in a 1.0 M NaCl solution buffered with 0.1 M Na_2HPO_4 and 0.1 M H_3BO_3 at 20°C as function of applied potential at pH 2.0 (black triangle), 3.0 (red circles), 4.0 (black circles), 5.0 (blue circles), 6.0 (red squares), 7.0 (black squares), 8.0 (blue squares). Solid lines serve as guides for the eye. The rate constants were extracted from leakage currents after applying potential steps to different potentials.

Results and Discussion

The potential dependence of the self-discharge rate constant at 20 °C is shown in Fig. 2. At low pH values there is an exponential dependence of the self-discharge rate constant with applied potential. This exponential increase of the self-discharge rate constant is accounted for by a self-discharge mechanism where a polymer intrinsic initial faradaic reaction leads to an unstable redox intermediate that reacts further by degradation of the polymer that we have previously reported (Scheme 1, upper reaction path).[35, 36] As evident from Fig. 2, an increased pH leads to higher over-all self-discharge rate constants. The increased pH also gives a less pronounced dependence of the applied potential indicating that the faradaic self-discharge is outcompeted at high pH by a parallel mechanism with a rate that depends on pH but not on applied potential (Scheme 1, lower reaction path).

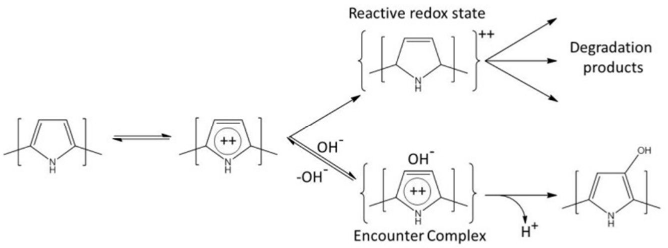

Scheme 1: Schematic illustration of the reaction paths leading to self-discharge in PPy. In the first reaction step the polymer is externally charged to a certain level of doping. From that state the polymer charge is consumed by two separate reaction paths, one of faradaic origin (upper path) and one by reaction with hydroxide ions (lower path).

At all pHs and temperatures the potential dependence of the observed rate constant could be described by an exponential dependence, i.e. $k = Ae^{bE}$, where A and b are fitted parameters and E is the applied potential (Fig. 2). In an attempt to separate the pH-dependent and the potential dependent rate constant of self-discharge, the potential dependence of the self-discharge rate was first fitted to a single exponential function, for each temperature separately. (This was done to minimize the experimental variation in each data point). The fitted potential dependence at pH 2 was then subtracted from the rate constants at other pH, and the result is shown in Fig. 3a. At low pH where the contribution from the pH-dependent reaction is close to negligible the subtraction in some cases resulted in negative rate constants. Negative rate constants have been omitted in figure 3a. For comparison, the potential dependence of the non-subtracted rate constants at pH 2 is shown in Fig 3b. It is clear that the subtracted rate constants (Fig. 3a), corresponding to the pH-dependent self-discharge mechanism only, are almost independent of applied potential. (It should be noted that the subtraction treatment relies on the faradaic self-discharge being independent of pH and on the assumption that the mechanisms operate independently of each other). Based on the independence on the subtracted rate constant (Fig. 3a) of applied potential a faradaic reaction can be excluded both as initial step and as rate limiting following step for this reaction as such reaction sequences would give an exponential dependence of applied potential as explained in detail in Ref. 36. The pH-dependent reaction mechanism is thus fundamentally different from the faradaic reaction mechanism that dominates at low pH (see below) and that has been investigated and presented previously.

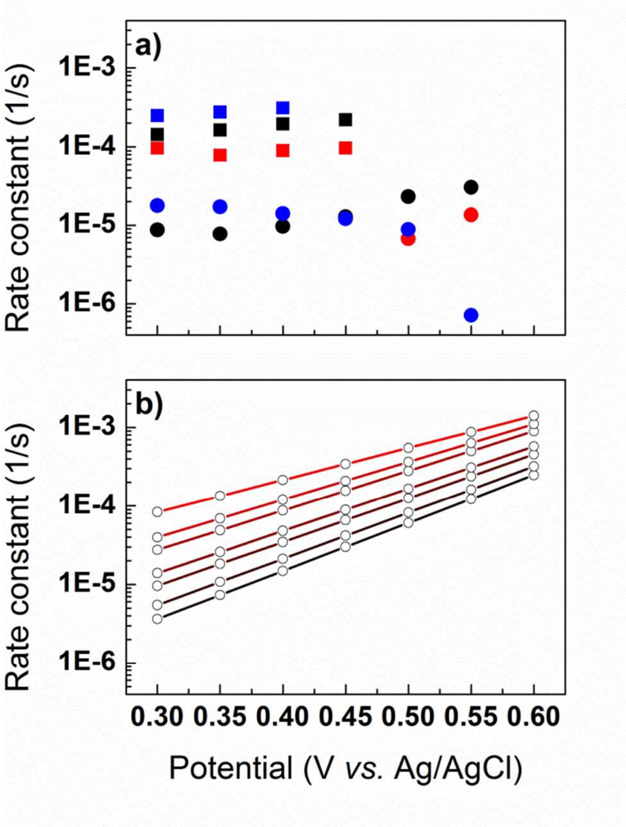

Figure 3. Evaluated rate constants as function of potential a) at pH 3.0 (red circles), 4.0 (black circles), 5.0 (blue circles), 6.0 (red squares), 7.0 (black squares), 8.0 (blue squares) at 20°C after subtraction of the pH 2 rate constants b) at pH 2 at 10°C, 20°C, 30°C, 40°C, 50°C, 60°C and 70°C. Higher temperatures are indicated with lighter red colours. While the rate constants at pH 2 shows a clear potential dependence the subtracted rate constants at high pH are independent of applied potential but strongly pH-dependent.

The pH-dependent mechanism is likely to comprise a nucleophilic attack by hydroxide ion which is a commonly proposed degradation path for conducting polymers in aqueous media.[37, 47-49] Based on extensive spectroscopic investigations, both on the system included in the present investigation[35, 50] as well as on other polypyrrole materials[42, 47-49, 51], it has been shown that nucleophilic attack on PPy by hydroxide ions results in addition of hydroxide to the pyrrole β-carbon. Such reaction requires close contact between the nucleophile and the polymer and, hence, the formation of an encounter complex [OH^--PPy^+] (Scheme 1, lower path).[25, 48] Irrespective of whether the reaction is diffusion controlled or activation controlled, i.e. if the reaction is kinetically limited by the formation of the encounter complex between polymer and hydroxide ion or by the reaction between the two reactants within the encounter complex, a linear dependence of the rate constant on hydroxide concentration is expected for such mechanisms. A linear correlation between the logarithm of the pH-dependent rate constant and pH was indeed observed. However, the slope was found to be 0.4 decades per pH indicating a somewhat more complicated reaction mechanism than a simple first-order reaction with respect to hydroxide ions which would give a slope of 1 decade per pH. (A similar reaction order with respect to hydroxide ions has previously been reported by Beck et.al.).[42, 43]

Considering the steady-state condition during the experiment the flux of hydroxide ions towards the polymer or through the material should be constant during the experiment and hence, in the case of a diffusion-limited reaction, the apparent rate constant is directly proportional to the diffusion coefficient. The diffusion coefficient, in turn, is directly proportional to the temperature according to the Stokes-Einstein equation. Much stronger temperature dependences are however observed experimentally, i.e. the logarithm of the apparent rate constant gives slopes of approximately 10 against the logarithm of the absolute temperature at all pH, making a diffusion limited reaction is unlikely.

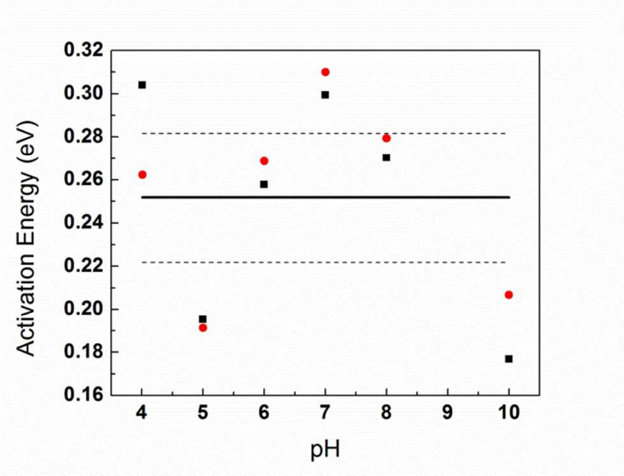

Figure 4. Activation energies for the pH-dependent reaction as function of pH at 0.35 (red circles) and 0.4 V (black squares). The solid line shows the average value for the activation energy and the dotted lines shows the 95 % confidence interval. The stochastic variation around the mean indicates that there is no systematic dependence on potential or pH of the activation energy.

If the pH-dependent reaction mechanism is instead assumed to be activation controlled, the temperature dependence of the rate constant is given by the activation barrier for the reaction of hydroxide with PPy, according to the Arrhenius equation, as well as the temperature dependence of the equilibrium constant for the formation of the encounter complex. The latter reaction is expected to have negative reaction entropy as the number of particles is reduced and hence the formation of the encounter complex will be disfavoured by increased temperatures. Moreover, as the mixing entropy of OH^- decreases with pH (by 59 meV/pH), making the reaction entropy successively less negative with increased pH, the negative temperature dependence on the over-all rate constant is expected to be more pronounced at low pH. None of these effects are observed experimentally and the temperature dependence of the equilibrium constant for the formation of the encounter complex is therefore considered to be negligible with respect to the over-all temperature dependence. The temperature dependence was therefore treated classically by the Arrhenius relation and the activation energy for the reaction was evaluated from the slope of the linear correlation between the logarithms of the rate constants as function of the inverse absolute temperature. The resulting activation energies at applied potentials of 0.35 V and at 0.40 V as function of pH is shown in Fig. 4. No correlation between neither pH nor potential and activation energy is observed. This is in clear contrast to the faradaic reaction that showed a linear correlation between applied potential and activation energy.[36] The difference in behaviour of the faradaic reaction and the pH-dependent reaction provides direct evidence for the proposed parallel mechanisms for self-discharge of PPy in aqueous media. Compared to the faradaic reaction the nucleophilic attack by hydroxide shows lower activation energies, i.e. 0.25 eV for nucleophilic addition compared to 0.5 eV for the faradaic reaction at comparable applied potentials.[36] Despite the lower activation barrier for the reaction with hydroxide ions the faradaic reaction dominates the self-discharge in the low-pH region.

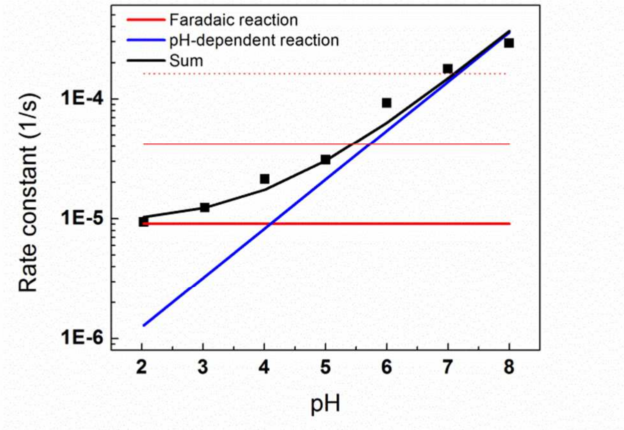

Figure 5. Experimentally determined rate constants for self-discharge at 0.35 V and 20°C as function of pH. The thick blue and red lines shows the contribution to the over-all rate constant from nucleophilic attack by hydroxide ions and from polymer intrinsic faradaic self-discharge respectively and the black line shows the sum of the two contributions. Thin red solid and dotted lines correspond to the rate constant for faradaic self-discharge at 0.45 V and 0.55 V respectively.

Fig. 5 shows the over-all rate constant for self-discharge at an applied potential of 0.35 V as function of pH together with the individual contributions to the self-discharge rate constant from the nucleophilic attack mechanism (in blue) and from the faradaic reaction (in red). At high pH (pH > 4) the pH-dependent reaction dominates while the faradaic reaction dominates at low pH. At pH 2, the rate constant for the faradaic reaction is one order of magnitude higher than the rate constant for the pH dependent reaction thus justifying the subtraction procedure for separating the two rate constants. At higher applied potentials the transition-pH is shifted to higher pH-values, as indicated in Fig. 5 by the thin red lines corresponding to the rate constant for the faradaic reaction at higher applied potentials, due to that the faradaic reaction rate increases with potential whilst the competing reaction is independent of potential. The faradaic reaction is also expected to be favoured by an increased temperature due to the higher activation energy for this reaction. To summarize; the self-discharge of PPy in aqueous media is composed of two mechanisms of fundamentally different origin. A faradaic reaction dominates at low pH while nucleophilic attack by hydroxide ions dominates at high pH.

Conclusions

We have shown that the self-discharge of oxidized PPy in a PPy-cellulose composite material in water solution is composed of two parallel self-discharge mechanisms, one of faradaic origin and one with characteristics of a reaction with hydroxide ions from the surrounding media. The faradaic reaction is characterized by a potential dependent rate constant and dominates the self-discharge at low pH and high applied potentials whilst the reaction with hydroxide ions dominates at high pH due to an exponential dependence of the corresponding rate constant with pH.

Acknowledgements

The authors thank the Swedish Foundation for Strategic Research (SSF), the Swedish Science Council (VR), the Bo Rydin Foundation, the European Institute of Innovation and Technology, under the KIC InnoEnergy NewMat project and the Swedish Energy Agency for their financial support of this work.

Notes and references

[a] Nanotechnology and Functional Materials, The Ångström Laboratory, Uppsala University, Box 534, 751 21 Uppsala, Sweden

1. N. Ferraz, D. O. Carlsson, J. Hong, R. Larsson, B. Fellström, L. Nyholm, M. Strømme and A. Mihranyan, *J. R. Soc. Interface*, 2012, **9**, 1943-1955.
2. A. Herland, K. M. Persson, V. Lundin, M. Fahlman, M. Berggren, E. W. H. Jager and A. I. Teixeira, *Angew. Chem. Int. Ed.*, 2011, **50**, 12529-12533.
3. K. M. Persson, R. Karlsson, K. Svennersten, S. Löffler, E. W. H. Jager, A. Richter-Dahlfors, P. Konradsson and M. Berggren, *Adv. Mater.*, 2011, **23**, 4403-4408.
4. R. H. Baughman, *Synth. Met.*, 1996, **78**, 339-353.
5. A. E. Abelow, K. M. Persson, E. W. H. Jager, M. Berggren and I. Zharov, *Macromolecular Materials and Engineering*, 2014, **299**, 190-197.
6. J. Joo and A. J. Epstein, *Appl. Phys. Lett.*, 1994, **65**, 2278-2280.
7. H. Klauk, *Chem. Soc. Rev.*, 2010, **39**, 2643-2666.
8. W. H. Kim, A. J. Mäkinen, N. Nikolov, R. Shashidhar, H. Kim and Z. H. Kafafi, *Appl. Phys. Lett.*, 2002, **80**, 3844-3846.
9. G. Li, V. Shrotriya, J. Huang, Y. Yao, T. Moriarty, K. Emery and Y. Yang, *Nat Mater*, 2005, **4**, 864-868.
10. U. Lange, N. V. Roznyatovskaya and V. M. Mirsky, *Anal. Chim. Acta*, 2008, **614**, 1-26.
11. M. Yun, N. V. Myung, R. P. Vasquez, C. Lee, E. Menke and R. M. Penner, *Nano Lett.*, 2004, **4**, 419-422.
12. D. Naegele and R. Bittihn, *Solid State Ionics*, 1988, **28–30, Part 2**, 983-989.
13. T. Osaka, S. Ogano, K. Naoi and N. Oyama, *J. Electrochem. Soc.*, 1989, **136**, 306-309.
14. W. Qiu, R. Zhou, L. Yang and Q. Liu, *Solid State Ionics*, 1996, **86–88, Part 2**, 903-906.
15. L. Yang, W. Qiu and Q. Liu, *Solid State Ionics*, 1996, **86–88, Part 2**, 819-824.
16. J. Wang, C. O. Too and G. G. Wallace, *J. Power Sources*, 2005, **150**, 223-228.
17. E. Frackowiak, V. Khomenko, K. Jurewicz, K. Lota and F. Béguin, *J. Power Sources*, 2006, **153**, 413-418.
18. Y. G. Wang, H. Q. Li and Y. Y. Xia, *Adv. Mater.*, 2006, **18**, 2619-2623.
19. H. Olsson, G. Nyström, M. Strømme, M. Sjödin and L. Nyholm, *Electrochem. Commun.*, 2011, **13**, 869-871.
20. L. Z. Fan, Y. S. Hu, J. Maier, P. Adelhelm, B. Smarsly and M. Antonietti, *Adv. Funct. Mater.*, 2007, **17**, 3083-3087.
21. L. L. Zhang, S. Li, J. Zhang, P. Guo, J. Zheng and X. S. Zhao, *Chem. Mater.*, 2009, **22**, 1195-1202.
22. G. Nyström, A. Razaq, M. Strømme, L. Nyholm and A. Mihranyan, *Nano Lett.*, 2009, **9**, 3635-3639.
23. L. Nyholm, G. Nyström, A. Mihranyan and M. Strømme, *Adv. Mater.*, 2011, **23**, 3751-3769.
24. P. Passiniemi and J. E. Österholm, *Synth. Met.*, 1987, **18**, 637-644.
25. P. Novák, B. Rasch and W. Vielstich, *J. Electrochem. Soc.*, 1991, **138**, 3300-3304.
26. P. Novák, K. Müller, K. S. V. Santhanam and O. Haas, *Chem. Rev.*, 1997, **97**, 207-282.
27. F. Rosciano, M. M. Salamone, R. Ruffo, M. Sassi and L. Beverina, *J. Electrochem. Soc.*, 2013, **160**, A1094-A1098.
28. C. Karlsson, H. Huang, M. Strømme, A. Gogoll and M. Sjödin, *J. Phys. Chem. C*, 2013, **117**, 23558-23567.
29. G. Milczarek and O. Inganäs, *Science*, 2012, **335**, 1468-1471.
30. L. Xu, *Electrochim. Acta*, 2014, **130**, 148-155.
31. T. L. Rose, A. B. Kon and F. Wang, *Abstr. Pap. Am. Chem. Soc.*, 1995, **209**, 311-312.
32. C. Karlsson, H. Huang, M. Strømme, A. Gogoll and M. Sjödin, *J. Phys. Chem. C*, 2014, **118**, 23499-23508.
33. C. Karlsson, E. Jämstorp, M. Strømme and M. Sjödin, *J. Phys. Chem. C*, 2012, **116**, 3793-3801.
34. C. Karlsson, A. Gogoll, M. Strømme and M. Sjödin, *J. Phys. Chem. C*, 2013, **117**, 894-901.
35. H. Olsson, E. Jämstorp Berg, M. Strømme and M. Sjödin, *Electrochem. Commun.*, 2015, **50**, 43-46.
36. H. Olsson, M. Strømme, L. Nyholm and M. Sjödin, *The Journal of Physical Chemistry C*, 2014, **118**, 29643-29649.
37. K. Qi, Y. Qiu, Z. Chen and X. Guo, *Corros. Sci.*, 2014, **80**, 318-330.
38. R. Mazeikiene and A. Malinauskas, *Polym. Degrad. Stab.*, 2002, **75**, 255-258.
39. Y. Li and R. Qian, *Electrochim. Acta*, 2000, **45**, 1727-1731.
40. S. Ghosh, G. A. Bowmaker, R. P. Cooney and J. M. Seakins, *Synth. Met.*, 1998, **95**, 63-67.
41. T. W. Lewis, G. G. Wallace, C. Y. Kim and D. Y. Kim, *Synth. Met.*, 1997, **84**, 403-404.
42. F. Beck, U. Barsch and R. Michaelis, *J. Electroanal. Chem.*, 1993, **351**, 169-184.
43. F. Beck and R. Michaelis, *Werkstoffe und Korrosion*, 1991, **42**, 341-347.
44. A. Mihranyan, A. P. Llagostera, R. Karmhag, M. Strømme and R. Ek, *Int. J. Pharm.*, 2004, **269**, 433-442.
45. H. Olsson, M. Sjödin, E. J. Berg, M. Strømme and L. Nyholm, *Green*, 2014, **4**, 27-39.
46. B. E. Conway, *Electrochemical Supercapacitors: Scientific Fundamentals and Technological Applications*, Springer, 1999.
47. A. A. Pud, *Synth. Met.*, 1994, **66**, 1-18.
48. D. S. Park, Y. B. Shim and S. M. Park, *J. Electrochem. Soc.*, 1993, **140**, 609-614.
49. F. Beck, P. Braun and M. Oberst, *Ber. Bunsen-Ges. Phys. Chem*, 1987, **91**, 967-974.
50. D. O. Carlsson, M. Sjödin, L. Nyholm and M. Strømme, *The Journal of Physical Chemistry B*, 2013, **117**, 3900-3910.
51. P. A. Christensen and A. Hamnett, *Electrochim. Acta*, 1991, **36**, 1263-1286.